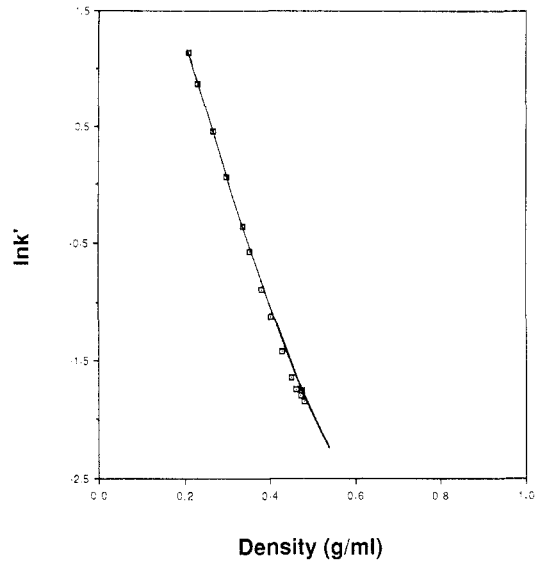

Figure 5. Plot of ln k' vs. density for napthalene at 55 °C (binary interaction parameter = 0.040 and $\bar{V}_1^{sp,\infty} = -125$ cm^3/mol): experimental (□) and calculated data (—).

tention. The slope of retention as a function of pressure is controlled by the fluid mobile phase and the intermolecular interactions between the solute and the stationary phase. Equation 5 can be used to predict solute retention once a k' value has been determined for the solute and the stationary phase. This could lead to enhanced speed and efficiency of selecting the appropriate conditions for a particular chromatographic separation for maximum selectivity and minimum separation time.

Particular conditions under which the predictive capability of the derived model could fail include sample overload of the column, such that one is working in the nonlinear region of the solute isotherm. Other areas of importance are specific solute–solvent interactions that are not accounted for by the particular EOS used in this work. These interactions include hydrogen bonding between the solvent and solute which could affect the standard mixing rules used in the calculation of the mixture parameters for $a(T)$ and b. Studies of solvatochromic shifts due to specific interactions are being explored to investigate such contributions.[16]

Conclusions

The understanding of the specific effects of the stationary phase and mobile phase on retention as pressure varies is necessary for a more complete understanding of retention in SFC. The thermodynamic approach described in this work allows prediction of solute retention as a function of pressure at constant temperature. The fluid mobile phase and stationary phase interactions control the rate of change of retention with pressure for simple solute molecules. For the mobile phase this control is expressed through the isothermal compressibility of the solvent and the partial molar volume of the solute. With simple molecular systems the intermolecular interactions between the solvent and solute can be approximated through simple binary mixing rules as seen for the calculation of $\bar{V}_1^{mp,\infty}$. The partial molar volume of the solute in the stationary phase suggests a possible attractive interaction between naphthalene and the stationary phase. The stationary phase for the case of biphenyl in SFC seems to play a less active role in the retention process, similar to the hydrophobic theory of solute retention in liquid chromatography.[17-19] For more complex cases, such as binary fluid mobile phases, or specific intermolecular interactions (i.e., hydrogen bonding, acid–base interactions), the simple binary mixing rules will most likely need to be modified.

Acknowledgment. The authors acknowledge the support of the U.S. Department of Energy, Office of Basic Energy Sciences, under Contract DE-AC06-76RLO 1830.

(16) Yonker, C. R.; Frye, S. L.; Kalkwarf, D. R.; Smith, R. D. *J. Phys. Chem.* **1986**, *90*, 3022.
(17) Horvath, C.; Melander, W.; Molnar, I. *J. Chromatogr.* **1976**, *125*, 129.
(18) Karger, B.; Grant, J. R.; Hartkopf, A.; Welner, P. *J. Chromatogr.* **1976**, *128*, 65.
(19) Horvath, C.; Melander, W. *J. Chromatogr. Sci.* **1977**, *15*, 393.

Melting and Other Phase Transformations of Oxygen from 120 to 650 K

J. Yen and M. Nicol*

Department of Chemistry and Biochemistry, University of California, Los Angeles, California 90024
(Received: October 21, 1986; In Final Form: February 9, 1987)

Direct observation and Raman spectra of molecular and lattice vibrations have been used to extend the melting curve of O_2 to more than 650 K and to determine many of the solid–solid phase boundaries from 119 to 650 K. The Raman spectra of the lattice vibrations between 3 and 8 GPa at temperatures below 200 K are suggestive of a new phase, ϕ-O_2, that may be stable between the fields of β-O_2 and δ-O_2. Four triple points have been located: fluid–β–ϵ at 645 ± 10 K and 16.3 ± 0.7 GPa; β–δ–ϵ at 368 ± 5 K and 11.5 ± 0.3 GPa; fluid–γ–β at 283 ± 4 K and 5.0 ± 0.3 GPa; and β–ϕ–δ at 200 ± 15 K and 6.3 ± 0.8 GPa. Above 645 K, large crystals of ϵ-O_2 suitable for X-ray diffraction studies can be grown from the fluid.

The homonuclear diatomic molecules form the simplest molecular solids. N_2, O_2, and F_2 have several molecular crystalline phases, and many of these phases share similar structures and other properties. Thus, several inter- and intramolecular interactions affect the structures, dynamics, stabilities, melting, and other properties of these solids. Measurements of these properties over a wide range of temperatures and densities and interpretation of the measurements in terms of atomic and molecular properties with quantitative statistical mechanical models might develop a detailed understanding of these interactions not only for diatomics but for molecular crystals in general.

This paper reports one set of such measurements: the phase relations and structures of the O_2 system at temperatures from 120 to 700 K to pressures near 20 GPa. The immediate motivation was the desire to determine the structure of the high-pressure ϵ phase.[1,2] Efforts to solve this structure by X-ray powder diffraction[3] or by growing crystals adequate for single-crystal dif-

(1) Nicol, M.; Hirsch, K. R.; Holzapfel, W. B. *Chem. Phys. Lett.* **1979**, *68*, 49.
(2) d'Amour, H.; Holzapfel, W. B.; Nicol, M. *J. Phys. Chem.* **1981**, *85*, 130.

0022-3654/87/2091-3336$01.50/0

fraction work from either β ($R\bar{3}m$)- or δ ($Fmmm$)-O_2 had been unsuccessful. Therefore, we decided to determine whether the stability field of the ϵ phase extended to the melting curve at pressure where single crystals of ϵ-O_2 could be grown. Detailed measurements of the melting, β–δ, δ–ϵ, and β–ϵ phase boundaries were made during stepwise heating and cooling runs with the high-pressure cell clamped at constant load to temperatures as high as 700 K and pressures in excess of 17 GPa. For each observation, the O_2 was allowed to equilibrate for at least 30 min after the temperature and/or pressure had settled at the new value and visual or spectroscopic observations indicated that the sample had ceased to change. Many of the phase changes observed during the studies at constant load were also confirmed by isothermal experiments during which the sample cell was slowly compressed or decompressed.

These experiments provided much new information about the O_2 system. (1) For the first time, the fluid–β–ϵ: triple point at 645 ± 10 K and 16.3 ± 0.7 GPa was determined. (2) Measurements along isotherms at intermediate temperatures demonstrate that the β–δ–ϵ triple point occurs between 343 and 373 K. Extrapolation of the β–δ, δ–ϵ, and β–ϵ boundaries measured in this study locates this triple point at 368 ± 5 K and 11.5 ± 0.3 GPa. (3) Raman spectra of the lattice modes at temperatures below 200 K observed in this and an earlier study[18] are suggestive of the existence of a new stable phase, designated here at as ϕ-O_2. At 123 K, ϕ-O_2 appears to be stable between 3.5 ± 0.3 GPa (the β–ϕ boundary) and 5.3 ± 0.1 GPa (the ϕ–δ boundary). A β–ϕ–δ triple point would occur approximately at 200 ± 15 K and 6.3 ± 0.8 GPa. (4) At pressures above 16 GPa, single crystals of ϵ-O_2 were grown from the melt. Although these conditions are extreme for high-pressure cells for single-crystal X-ray work, Schiferl and Zinn have used these results to grow a single crystal of ϵ-O_2 in a modified Merrill–Barrett cell.[4] The rest of the section reviews previous work on the O_2 phase diagram with emphasis on temperatures above 100 K. The equipment and techniques used for these studies and the observations are described in detail in subsequent sections.

Background

Studies of the phase diagram of O_2[1-3,5-18] can be divided into three temperature ranges: (1) 100–300 K, (2) below 100 K, and (3) above 300 K. Between 100 and 300 K to 50 GPa, there is general agreement about most of the equilibrium phases, although some issue about structures and the low-temperature region between β- and ϵ-O_2 are incomplete. This agreement is summarized in the phase diagram shown in Figure 1 of ref 3, which also indicates the convention for naming the phases with Greek letters that is used in this report. In addition to the fluid (and vapor near atmospheric pressure at low temperatures), two solid phases, γ (P_{m3n}) and β ($R\bar{3}m$), occur at low pressures and are stable at atmospheric pressures at lower temperature. Two other solid phases, δ ($Fmmm$) and ϵ (unknown structure, probably an orthorhombic distortion of δ), are well established at higher pressures. These four solids can be clearly distinguished from each other by color, vibrational spectra, and X-ray diffraction patterns. The transformations among these solids are clearly first-order. Two other metastable phase, χ-O_2 and ω-O_2, have been identified in powder X-ray diffraction patterns obtained near 300 K by Olinger et al.,[3] and Raman evidence that suggests the existence of another low-temperature phase, ϕ-O_2, is described below.

X-ray diffraction patterns of β-, δ-, and α ($C2/m$)-O_2 [which is stable only at low temperatures and pressures] and less direct evidence for ϵ, ϕ, χ, and ω suggest that these phases have layered structures and differ qualitatively from the highly disordered γ-O_2. The principal differences among the layered phases appear to involve the ordered molecular arrangements within the layers, although the stacking of the ordered layers also may distinguish among these phases. Single-crystal diffraction data for β-O_2 near 6 GPa and 300 K[2] indicate, for example, that the stacking of the layers is disordered except for adjacent layers. Whether the disorder persists at lower temperatures or higher pressures is unknown. X-ray observations suggest that more ordered polytypes with the intralayer structure of β-O_2 occur.[2,3] d'Amour's diffraction pattern of a single crystal at 8 GPa and 300 K indicated that its c axis was 6 times the interlayer separation,[2] that is, twice as long as the c axis of the conventional β-O_2 structure. Olinger, Mills, and Roof[3] suggest that χ-O_2 is a hexagonal ($P6_3/m$ or $P6_3$) varient of β-O_2. χ-O_2 was found together with β-O_2 at room temperature when the pressure on δ-O_2 crystals was lowered by as much as 2 GPa below the β–δ boundary. Unfortunately, no spectroscopic signatures that distinguish χ-O_2 from β- or δ-O_2 have been identified, and the occurrence of χ-O_2 at other than room temperature has not been studied.

The ω phase has been detected only as four diffraction lines in powder patterns obtained by Oliger et al.[3] and then only coexisting with δ- or ϵ-O_2 near 11.5 ± 0.5 GPa at 300 K. These four lines could not be indexed satisfactorily, so that the structure of this phase is essentially unknown. No spectroscopic observations have been associated with these X-ray data.

The studies described here did not extend below 100 K; thus, other work in this region will only be summarized. Four solid phases seem to be well established: at low pressures, α, β, and γ and, above 7.8 GPa, ϵ. Jodl, Boldnan, and Hocheimer[18] have reported Raman data from which they conclude that two other phase, $\bar{\alpha}$-O_2 (from 0.6 to 3 GPa) and δ-O_2 (from 3 to 8 GPa), are stable below 100 K between α- and β-O_2 at low pressures and ϵ-O_2 at high pressures. The graph of vibrational frequencies vs. pressure at 80 K in Figure 3 of ref 18 however, is not inconsistent with an alternative interpretation, described below, which places the lower limit of the stability field of δ-O_2 between 5 and 6 GPa and inserts a new phase, ϕ-O_2, between δ-O_2 and either β-O_2 or, below 100 K, Jodl, Boldnan, and Hocheimer's $\bar{\alpha}$-O_2.

At temperatures above 300 K, only two limited sets of observations have been published.[2,11] These sets differ significantly from each other; see ref 3, Figure 2. Some of the differences result because the laser used by Nicol et al.[1] heated the samples. The true temperatures of these samples, therefore, were somewhat higher than the measured temperatures of the surrounding gasket, cell, and Pt resistance thermometer.

This systematic error was avoided by Yagi, Hirsch, and Holzapfel,[11] who detected the phase transformations visually while varying the temperature of the sample at an unspecified rate along an approximately isochoric path. At a given pressure, Yagi et al.[11] observed melting and the β–δ and δ–ϵ transformations at higher temperatures than Nicol et al.[1] However, the temperature differences along the melting line (between two nearly colorless phases) were about as large as the difference along the δ–ϵ boundary at higher pressures. Since δ and ϵ absorbed strongly, laser heating would be expected to be more important at the δ–ϵ transition. This suggests that a second factor contributed to the temperature difference.

(3) Olinger, B.; Mills, R. L.; Roof, Jr., R. B. *J. Chem. Phys.* **1984**, *81*, 5068.
(4) Schiferl, D.; Zinn, A. S., personal communication.
(5) Giauque, W. F.; Johnson, H. L. *J. Am. Chem. Soc.* **1929**, *51*, 2300.
(6) Mills, R. L.; Grilly, E. R. *Phys. Rev.* **1955**, *99*, 480.
(7) Stevenson, R. *J. Chem. Phys.* **1957**, *27*, 673.
(8) Stewart, J. W. *J. Phys. Chem. Solids* **1959**, *12*. 97.
(9) Meier, R. J.; Schinkel, C. J.; deVisser, A. *J. Phys. C* **1982**, *15*, 1015.
(10) Syassen, K.; Nicol, M. In *Physics of Solids under High Pressure*; Schilling, J. S., Skelton, R. N., Eds.; North-Holland: New York, 1981; p 33.
(11) Yagi, T.; Hirsch, K. R.; Holzapfel, W. B. *J. Phys. Chem.* **1983**, *87*, 2272.
(12) Yen, J.; Nicol, M. *J. Phys. Chem.* **1983**, *87*, 1045.
(13) Meier, R. J.; van Albada, M. P.; Lagendijk, A. *Phys. Rev. Lett.* **1984**, *52*, 1045.
(14) Schiferl, D.; Cromer, D. T.; Mills, R. L. *Acta Crystallogr. Sect. B: Struct. Crystallogr. Cryst. Chem.* **1981**, *37*, 1329.
(15) Swanson, B. I.; Agnew, S. F.; Jones, L. H.; Mills, R. L.; Schiferl, D. *J. Phys. Chem.* **1983**, *87*, 2463.
(16) Schiferl, D.; Cromer, D. T.; Schwalbe, L. A.; Mills, R. L. *Acta Crystallogr. Sect. B: Struct. Sci.* **1983**, *39*, 53.
(17) Stepherns, P. W.; Birgenau, R. J.; Majkrzak, C. F.; Shirani, E. *Phys. Rev. B: Condens. Matter* **1983**, *28*, 452.
(18) Jodl, H. J.; Boldnan, F.; Hocheimer, H. D. *Phys. Rev. B: Condens. Matter* **1985**, *31*, 1015.

A possibility is that Yagi et al. did not measure the temperature at the sample directly but computed it from the temperature measured by a thermocouple on one of the diamonds and corrected for temperature gradients. The corrections were determined in separate experiments by replacing the sample with a thermocouple. The temperature gradients may have been changed by this substitution, and the gradients or kinetics of the transformations also may depend upon heating rates. For these reasons, great emphasis was placed in the present study on keeping the powers of the exciting lasers to a minimum and to varying the temperature and pressure of the sample very slowly.

Experimental Section

These measurements were made in the diamond-anvil high-pressure cell and cryostat of Holzapfel's design[19] used for the earlier study of the oxygen phase diagram at lower pressures and temperatures.[12] Inconel 718 or, above 470 K, 301 stainless steel gaskets were used to confine the sample between diamond anvills with 0.5-mm culets. Each gasket was preindented to a thickness between 70 and 100 μm and was drilled with a 200-μm or, above 470 K, 150-μm diameter hole for the sample. The techniques for heating the cell and procedures for determining the temperatures, pressures, and oxygen phases were selected in order to approach equilibrium carefully, especially near phase boundaries.

For most of the measurements, the cell was clamped at a fixed setting of the load generating mechanism and was mounted in a massive copper block. For low temperatures, the upper surface of the copper block was mounted directly to the liquid nitrogen reservoir of the cryostat, and the block was heated electrically by two 100-W cartridge heaters. The heating was regulated by sensing the temperature of near the middle of the block with VECO 05A7 or 1-EA thermistors that controlled the operation of the power supply (UCLA Chemistry and Biochemistry Electronics Shop Model 3819A) for the heater. With this method, the temperature fluctuations at the sample could be kept within ±1 K.

For high temperatures, the block was suspended in the vacuum cryostat by only two stainless steel screws in order to minimize thermal contact with the surroundings. The temperature of the cell was then varied under approximately isobaric conditions by adjusting the set point of an Omega Model 158-713 proportional temperature controller which sensed the temperature of a copper–constantan thermocouple mounted in the copper block and powered two cartridge heaters mounted in the copper block. With this arrangement, the temperature of the cell could be maintained within ±1 K. Above 525 K, a 75- or 100-W heating tape was wrapped around the block for additional base line heating.

The temperatures of the samples were determined by measuring the temperature of the gasket with both (1) a copper–constantan thermocouple sensed by an Omega 410A digital readout and (2) a second copper-jacketed Pt resistance thermometer whose resistance was measured with a Fluke digital multimeter. Wakefield No. 120-8 thermal compound as well as mechanical force was used to maintain thermal contact among these sensors and the gasket. During any measurement, the temperature sensed by these two thermometers agreed within ±0.5 K at temperatures below 423 K, ±1.5 K between 423 and 523 K, and ±2.5 K at higher temperatures. These were also about the ranges over which the measured temperatures fluctuated over periods of minutes, although fluctuations as large as 4 K were observed in some experiments.

Pressures were determined by measuring the difference in wavelength between the intensity maxima of the R_1 luminescence of a small chip from a ruby inside the high-pressure chamber and of a larger chip of the ruby at the same temperature at atmospheric pressure. The spectra were excited with the 515-nm line of an argon ion laser or, below room temperature, the 647-nm line of a krypton ion laser. In order to minimize heating of the sample during these measurements, the exciting lasers were operated at low powers, and the excitation was only loosely focused. Below room temperature, the power of the laser at the sample was estimated to be less than 5 mW for argon excitation or 35 mW for krypton excitation. Higher excitation powers were necessary above room temperatures. However, the power was kept below 15 mW below 470 K and 50 mW at higher temperatures.

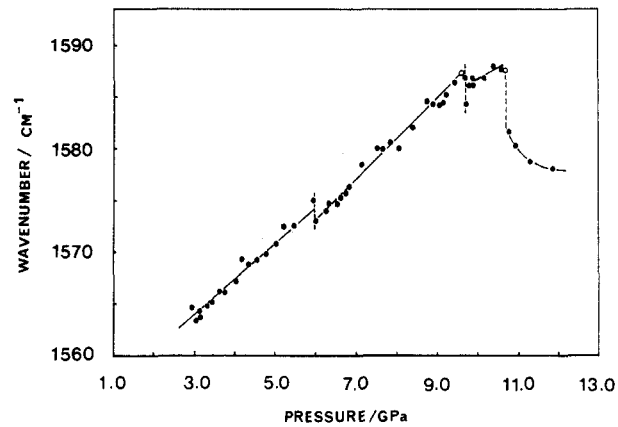

Figure 1. Pressure dependence of the wavenumbers of the O_2 stretching line in Raman spectra at 323 K. Broken vertica lines denote the melting, β–δ, and δ–ϵ transitions at 6.1, 9.7, and 10.7 GPa.

At any temperature, the pressure was computed by multiplying the wavelength shift by the factor 2.746 GPa/nm. The nonlinearity of the shift that has been established at rom temperature was ignored because the correction is relatively small at pressures of interest here and, moreover, has not been established at other temperatures. Pressures determined by this method are estimated to have a precision of ±0.3 GPa at temperatures below 593 K and ±0.7 GPa at higher temperatures.

The phases in the O_2 samples often were identified visually, but many identifications were confirmed by Raman spectra that were taken during isothermal compression–decompression cycles or heating–cooling cycles under approximately isochoric conditions. Various Spectra-Physics argon and krypton ion lasers were used for excitation. The lasers were typically operated at less than 50 mW, unfocused, at the sample and never more than 200 mW for weak signals from small samples at higher temperatures and pressures. Raman spectra were collected with a Spex 1400 double monochromator and photon-counting detection system. During these isothermal studies, the cell was allowed to equilibrate for 20–30 min after each adjustment of the load on the cell. Then, the pressure was measured, the Raman spectrum was recorded, and the pressure was remeasured. If the pressure changed during the Raman spectrum, the process of equilibration, pressure determination, and collecting the Raman spectrum was repeated. During the visual observations, the criteria for equilibration included both a 20–30-min delay after adjusting the pressure or temperature and, subsequently, no observed change of the appearance of the sample. Under these conditions, the phase boundaries determined from the laser Raman data did not differ significantly from boundaries determined by direct observations; see Figure 8.

Results

Figures 1–6 are plots of the wavenumber shifts of the O_2 stretching mode of the Raman spectrum vs. pressure measured during isothermal compression–decompression experiments at 323, 343, 373, 463, 123, and 223 K. The observations at 323 K in Figure 1 are similar to the room-temperature data in ref 1. In three regions that correspond to the fluid, β, and δ phases, the vibrational frequency increases essentially linearly with increasing pressure by 3.7, 3.4, and approximately 2 cm^{-1}/GPa, respectively. Slopes and intercepts at zero pressure determined by fitting the data for the fluid and β phases to linear representations of the pressure dependences of the wavenumbers of the O_2 stretching mode at this and other temperatures are summarized in Table I. Discontinuities in these lines coincide with phase transitions at 6.1, 9.7, and 10.7 GPa. The nonlinear pressure dependence

(19) Hirsch, K. R.; Holzapfel, W. B. *Rev. Sci. Instrum.* **1981**, *52*, 52.

TABLE I: Slopes and Zero-Pressure Intercepts Determined by Least-Squares Fits of the Linear Pressure Dependence of the O_2 Stretching Modes for the Fluid and β Phases at Four Temperatures

phase	temp, K	ν_0, cm^{-1}	$\partial\nu/\partial P$, cm^{-1} GPa^{-1}
fluid	223	1549	3.3_5
	323	1552	3.7_0
	373	1554	3.3
	463	1549	3.3
β	223	1553	3.2_3
	323	1554	3.4_5
	373	1556	3.1
	463	1555	3.0

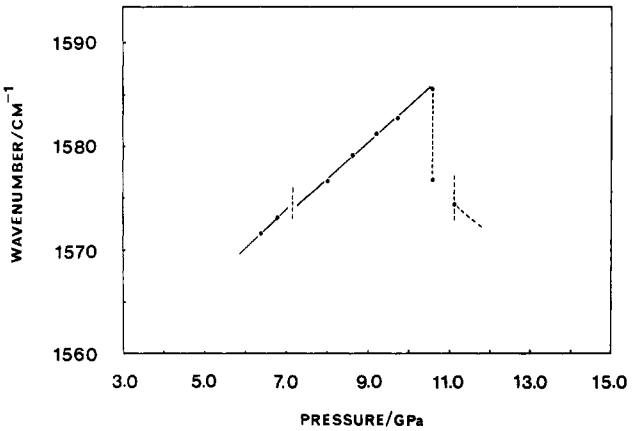

Figure 2. Pressure dependence of the wavenumbers of the O_2 stretching line in Raman spectra at 343 K. Broken vertical lines denote the melting, β–δ, and δ–ϵ transitions which were determined by visual observations to be at 7.0, 10.6, and 11.1 GPa.

of the stretching frequency in ϵ-O_2 is apparent just above the δ–ϵ boundary. These observations with low excitation powers prove that the β–δ–ϵ triple point is higher than 323 K and demonstrate that laser heating significantly influenced the results reported by Nicol et al.[1] The phase boundaries determined from the isothermal Raman experiments at this and other temperatures are plotted as open circles in Figure 8.

The limited number of observations at 343 K shown in Figure 2 hint at the difficulties involved in using Raman data to detect phase transitions in O_2 near this temperature. The pressure dependence of the stretching frequency in β-O_2 is greater than in the fluid, and the temperature dependence is negligible. Thus, near 7.0 GPa, the wavenumber shift of the stretching mode is the same for the fluid and β phases. Although the line is broader in the fluid phase, the narrow slits or long integration times needed to determine the precise line shapes with a scanning monochromator and low excitation powers make line width determinations tedious. The limited range of stability of δ-O_2 at this temperature and the need to avoid laser heating also precluded detailed examination of the β–δ–ϵ region at this temperature by Raman spectra.

By 373 K, the δ phase disappears. Only three phases, fluid, β, and ϵ, are detected in the data shown in Figure 3. The melting pressure is 8.0 GPa. At this point, the stretching frequency is lower in the fluid than in β-O_2. The β–ϵ transition occurs at 11.8 GPa.

A limited number of Raman measurements at 463 K are summarized in Figure 4. Discontinuities are apparent at the melting (10.7 GPa) and β–ϵ (13.2 GPa) transitions. Very detailed spectroscopic work was impractical at this and higher temperatures. Small samples (<100-μm diameter) in thin (<50 μm) gaskets had to be used to prevent blowouts, and the Raman spectra of these samples were too wide and weak for rapid collection.

A 123 K isotherm of the O_2 stretching mode is shown in Figure 5. These data were compiled from several sets of isochoric heating–cooling cycles and suggest that four phases occur between 0.8 and 10 GPa. The two-line spectrum of γ-O_2 is observed below 1.4 GPa,[12] β-O_2 is detected between 1.4 and 3.5 GPa, and ϵ-O_2

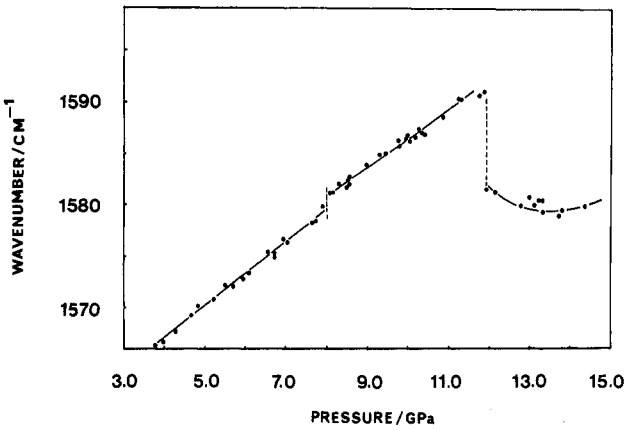

Figure 3. Pressure dependence of the wavenumbers of the O_2 stretching line in Raman spectra at 373 K. Broken vertical lines denote the melting and β–ϵ transitions at 8.0 and 11.8 GPa.

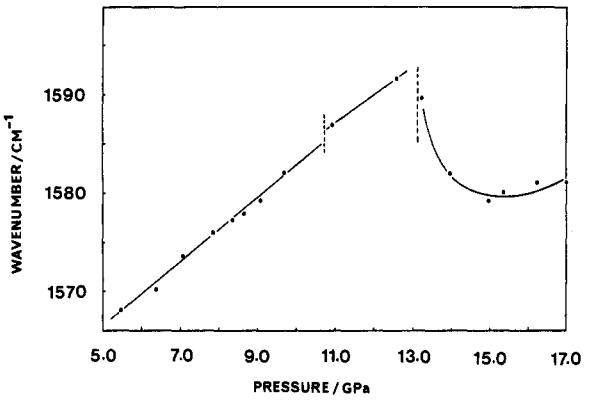

Figure 4. Pressure dependence of the wavenumbers of the O_2 stretching line in Raman spectrum at 463 K. Broken vertical lines denote the melting and β–ϵ transitions at 10.7 and 13.2 GPa.

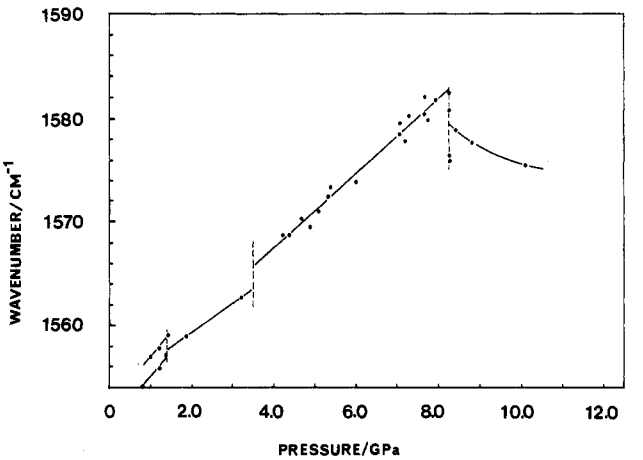

Figure 5. Pressure dependence of the wavenumbers of the O_2 stretching line in Raman spectra at 123 K. Broken vertical lines denote transitions at 1.4 [γ–β], 3.5 [β–ϕ(?)], and 8.3 [δ(?)–ϵ] GPa.

appears above 8.8 GPa. The relatively continuous and appearently linear pressure dependence of this vibron mode between 3.5 and 8.8 GPa suggests that one phase, presumably δ-O_2, is stable under these conditions. However, observations at 223 K shown in Figure 6 and Raman spectra of the lattice vibrations at temperatures between 120 and 200 K (discussed below) imply that the assignment of this field as δ-O_2 may not be correct.

The 223 K isotherm in Figure 6 shows the expected behavior for the fluid (below 2.75 GPa), γ-O_2 (2.75–3.85 GPa), β-O_2 (3.85–7.1 GPa), and ϵ-O_2 (above 9.3 GPa). However, an unusual *negative* pressure dependence of this O_2 mode was observed between approximately 7.5 and 9.3 GPa. For purposes of this report, this region is labeled δ-O_2. However, this result suggests that the

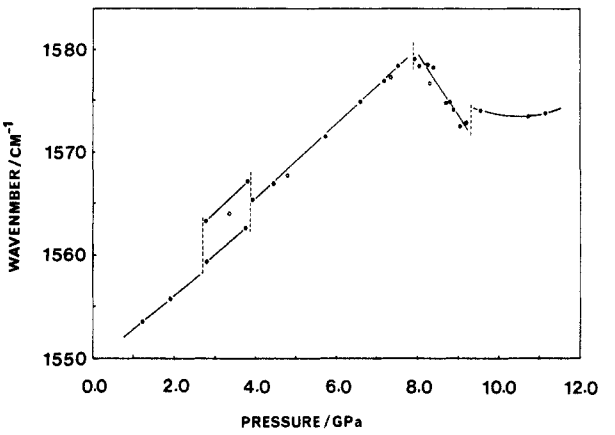

Figure 6. Pressure dependence of the wavenumbers of the O_2 stretching line in Raman spectra at 223 K. Broken vertical lines denote transitions at 2.75 [melting], 3.85 [γ–β], 7.5 [β–δ(?)], and 9.3 [δ(?)–ϵ] GPa.

stable phase in this region may not be δ-O_2. More studies over a finer grid of temperatures and pressures are needed to resolve this issue.

Figure 7 depicts four of many Raman spectra of lattice modes that were taken during heating–cooling cycles under constant applied loads from 120 to 160 K or higher temperatures. These spectra were obtained with one O_2 sample and represent similar effects observed with other samples. The available instruments and use of low excitation powers made it difficult to obtain good spectra of the lattice modes. Nevertheless, the major results appeared to be reproducible. The spectrum at 8.3 GPa attributed to ϵ-O_2 is similar to the spectrum of ϵ-O_2 at 80 K reported by Jodl et al.[18] The strong 142-cm^{-1} and weaker 200-cm^{-1} features of the 5.2-GPa spectrum resemble the spectrum of δ-O_2 described by the same authors; similar features occur in the 6.2-GPa spectra. Like many low-temperature spectra, the 6.2-GPa spectrum also includes a weak band of moderate width near 121 cm^{-1}; the frequent occurrence of bands between 120 and 125 cm^{-1} at these pressures and temperatures suggests that they are real and may be related to δ-O_2 or some other phase that coexists with δ-O_2.

The wavenumber of the most intense band in the spectra of the lattice modes of δ-O_2 can be represented as

$$\nu/\mathrm{cm}^{-1} = 45 + 17.6(P/\mathrm{GPa}) \quad (1)$$

between 5.2 and 8.1 GPa at 123 K. Within the precision of the measurements, the wavenumbers of this band appear to be independent of temperature. On this basis, the positions of the strong 123-cm^{-1} band in the 4.9-GPa spectrum and of similar bands in other low-temperature spectra between 3.5 and 5 GPa are significantly lower, and vary about half as rapidly with pressure, than given by eq 1. Although these observations are not unambiguous, they strongly suggest that, below 200 K, the position of the intense band in the Raman spectrum of the lattice modes shifts discontinuously slightly above 5 GPa. The spectra at 80 K reported by Jodl et al. also can be interpreted on this basis.

The most plausible explanation for a discontinuity at this pressure would be that another phase occurs between β-O_2 and about 5 GPa at temperatures below 200 K. The weak band near 123 cm^{-1} in spectra between 5 and 8 GPa may indicate that this new phase coexists with δ-O_2 in some samples at higher pressures. There is no direct evidence to connect this new phase with χ, ω, or other reported phases of O_2; thus, it is arbitrarily designated ϕ-O_2 for this report. The ϕ–δ boundary determined on the basis of this interpretation and available Raman spectra is shown in Figure 8. Extrapolation of this boundary to the β–ϕ and β–δ boundaries suggests that the β–ϕ–δ triple point is at 200 ± 15 K and 6.3 ± 0.8 GPa.

The phase transitions located by Raman spectroscopy (open points) in this and our earlier studies of O_2 are plotted together with representative data for transitions located visually (filled points) in Figure 8. At temperatures and pressures where both methods were used, there are no obvious differences between the data. Above 463 K, only visual techniques and relatively thin samples were used. The fluid, β, and ϵ phases were readily identified by changes from nearly colorless to yellow and to red with increasing pressure. Selected values of the transition parameters are listed in Table II.

At 645 K, the highest temperature studied carefully, no intermediate yellow phase was observed during several repeated crossings between the liquid and ϵ phases near 16.3 GPa. Extrapolation of observations from lower temperatures suggests that the fluid-β–ϵ triple point is at or slightly below this pressure and temperature. At this and higher temperatures and pressures, single crystals of ϵ-O_2 can be grown from the fluid.

TABLE II: Temperature and Pressures of Oxygen Phase Transitions Determined in This Study[a]

phase	temp,[b] K	press.,[c] GPa
fluid–γ	133	1.0$_5$
	150	1.3
	170	1.6
	185	2.0
	203	2.3
	223	2.8
	252	3.9
	273	4.7
fluid–β	285	5.3
	323	6.1
	373	7.9
	402 ± 4	8.6
	425	9.1
	463	10.7
	500	11.2
	531	12.6
	573	13.7
	608	15.1
fluid–ϵ	645	16.7
γ–β	119	1.2
	138	1.6
	155	2.1
	185	2.7
	202	3.2
	222	3.6
	268	5.0
	280	5.1
β–ϕ	123	3.5
	150	4.4
	165	4.9
	180	5.8
ϕ–δ	123 ± 4	5.3
	133	5.4
	143	5.5–5.9
β–δ	215	6.9
	226	7.5
	248	7.9
	323	9.7
	343	10.6
δ–ϵ	123	8.3
	223	9.4
	293	10.5
	323	10.8
	343	11.1
	373	11.9
β–ϵ	398	12.1
	425	12.5
	463	13.2
	503	14.1
	544	15.0
	573	15.4
	594	16.0

[a] When multiple determinations were made by visual and Raman observations, the data have been averaged. A complete listing of all determinations is available in Yen, J. Doctoral Dissertation, University of California, Los Angeles, 1986, which can be obtained from University Microfilms, Ann Arbor, MI. [b] Unless indicated, the uncertainties of these temperatures are estimated to be ±0.5 K below 423 K, ±1.5 K from 423 to 523 K, and ±2.5 K at higher temperature. [c] Unless indicated, the uncertainties of these pressures are estimated to be ±0.3 GPa below 593 K and ±0.7 GPa at higher temperatures.

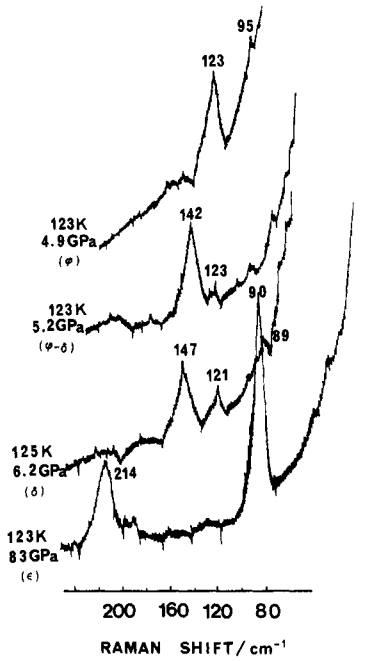

Figure 7. Partial Raman spectra of the lattice modes of solid O_2 near 123 K. The spectra are assigned to the various O_2 phases as follows: ϕ, 4.9 GPa; δ, 5.2 and 6.2 GPa; ϵ, 8.3 GPa.

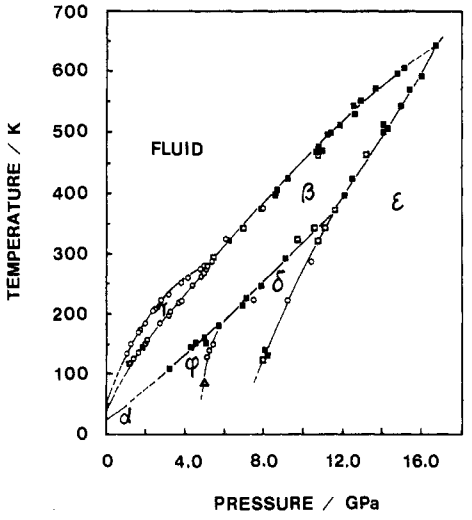

Figure 8. Established phase diagram of O_2 from 100 to 700 K at pressures to 17 GPa. Data represented by open and closed points were determined by Raman spectroscopy and visual observations, respectively. The solid lines have been drawn by hand through these data and represent our best estimates of the phase boundaries.

The Raman data cited above bound the temperature of the β–δ–ϵ triple point between 343 and 373 K. Our best estimates based upon extrapolation of our visual and Raman measurements for the β–δ, δ–ϵ, and β–ϵ transitions suggest that the triple point is at 368 ± 5 K and 11.5 ± 0.3 GPa. As shown in Figure 9, these

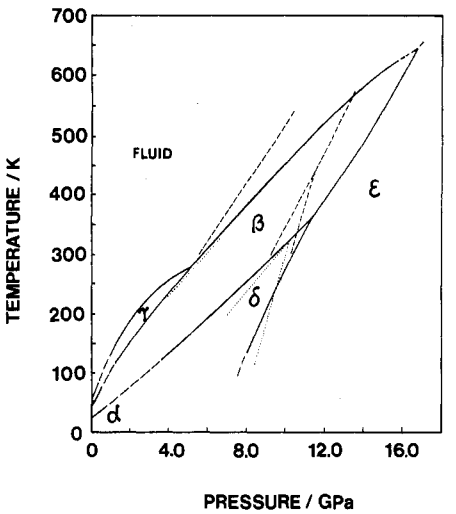

Figure 9. Comparison of the phase boundaries determine in this study (—) with boundaries reported previously by Nicol, Hirsch, and Holzapfel[1] (···) and by Yagi, Hirsch, and Holzapfel[11] (- - -). As described in the test, the differences are attributed to effects of laser heating of δ- and ϵ-O_2 on the temperatures reported in ref 1 and to imprecise corrections for differences between the temperatures of the sample and thermocouples during the thermal scans made in ref 11.

values are somewhat higher than given in the initial report of δ-O_2 by Nicol et al.,[1] which is consistent with the role of laser heating in that study. This pressure is the same, but this temperature is more than 70 K lower than the values reported by Yagi et al.[11] It must be remembered, however, that neither the Raman spectra nor visual appearances of χ- or ω-O_2 have been characterized. Thus, the influence of these structures or of possible β-O_2 polytypes on these determinations of the β–δ–ϵ phase boundaries has not been determined. Studies involving Raman, visual, and X-ray diffraction analyses of the same sample are needed to resolve this uncertainty.

Finally, it should be noted that the pressure dependence of the melting temperature for O_2 (~40 K/GPa) is significantly smaller than for H_2, N_2, or F_2. Young et al.[20] have considered the origins of the differences and conclude that the principal contribution to the differences is a higher degree of orientational order in solid O_2.

Acknowledgment. It is a pleasure to acknowledge valuable assistance provided by K. Ahzez, A. Chopelas, D. Kliner, and A. Koumvakalis and informative discussions with D. Schiferl, D. A. Young, and A. S. Zinn. This work was supported by National Science Foundation Grant DMR83-18812.

Registry No. O_2, 7782-44-7.

(20) Young, D. A.; Zha, C.-S.; Boehler, R.; Zinn, A. S.; Yen, J.; Nicol, M.; Schiferl, D.; Kincaid, S.; Hanson, R. C.; Pinnick, D., *Phys. Rev. B: Condens. Matter*, in press.